A Probabilistic Model of Hypobaric Decompression Sickness Based on 66 Chamber Tests

JOHNNY CONKIN, Ph.D., M.S., K. VASANTHA KUMAR, M.D., M.B., MICHAEL R. POWELL, Ph.D., M.S., PHILIP P. FOSTER, M.D., M.S., and JAMES M. WALIGORA, M.S., B.S.

CONKIN J, KUMAR KV, POWELL MR, FOSTER PP, WALIGORA JM. *A probabilistic model of hypobaric decompression sickness based on 66 chamber tests.* **Aviat Space Environ Med 1996; 67:176–83.**

One consequence of the NASA tissue ratio (TR) model is that calculated probability of decompression sickness [P(DCS)] is constant in tests at different ambient pressures so long as the ratio of $P1N_2$ to P2 is the same in each test; $P1N_2$ is N_2 pressure in the 360 minute half-time compartment, and P2 is ambient pressure after decompression. We test the hypothesis that constant P(DCS) is better described by TRs that decrease as P2 decreases. Data were from 66 NASA and USAF hypobaric chamber tests resulting in 211 cases of DCS in 1075 exposures. The response variable was presence or absence of DCS while at P2. Explanatory variables were $P1N_2$, P2, exercise at P2, (yes or no), time to DCS (failure time), and time to end of test in those without DCS (censored time). Probability models were fitted using techniques from survival analysis. The log likelihood for the two parameter log logistic survival model was −846 with only failure and censored times, −801 when TR [$P1N_2$/P2] plus exercise were added, and −663 when modified TR [$(((P1N_2 + c1)/P2) - 1)^{c2}$] plus exercise were added, where c1 and c2 are fitted parameters in the five parameter model. Constant P(DCS) was better described by TRs that decrease as P2 decreases; a conclusion supported by additional empirical observations, and bubble growth models that are independent of DCS data. Exercise increased the P(DCS) at P2. As a description of decompression "dose", the modified TR was superior to TR over a wider range of experimental conditions.

ASTRONAUTS OR COSMONAUTS who perform extravehicular activities (EVA's), also called space walks, from the U.S. Shuttle, Russian Mir, and any future space station are at risk of getting decompression sickness (DCS). The decrease in ambient pressure from P1, the 14.7 pounds per square inch absolute (psia) shuttle cabin pressure, to P2, the 4.3 psia space suit pressure, may cause signs and symptoms of DCS if: a) tissue nitrogen (N_2) partial pressure is not reduced through adequate denitrogenation before the decompression (17); b) the EVA is of long duration; and c) the astronaut works vigorously during the EVA.

This report documents an approach to estimate the risk or probability of DCS [P(DCS)] in future EVA's given information about: a) the denitrogenation prior to the decompression; b) magnitude of the decompression; c) exercise after the decompression; and d) length of the EVA. The analysis is based on results from previous hypobaric chamber tests, and accounts for failure and censored times. Failure time is defined as the elapsed time from the beginning of a test after the decompression to the first report of a DCS symptom. Censored time is the elapsed time from the beginning of a test after the decompression to the scheduled end of the test, also called right censored time (1,7,9,10). A model that includes failure and censored times improves on previous efforts to estimate the probability of hypobaric DCS (6,11).

Other approaches to estimate the P(DCS) have been explored (4,6,8,9,11,16). An initial effort at the Johnson Space Center was to define a decompression dose as $[(P1N_2/P2) - 0.78]$, where $P1N_2$ is N_2 partial pressure in a theoretical 360 min half-time compartment. The dose was optimized to 927 dichotomous DCS responses by estimating the two parameters of the Hill equation using the maximum likelihood method (4) to provide a probability model. One consequence of the NASA model is that calculated P(DCS) is constant in tests at different altitudes (P2's) so long as the ratio of $P1N_2$ to P2, the tissue ratio (TR), is the same in each test. We define constant P(DCS) as any combination of variables that produce the same cumulative risk will always produce the same P(DCS). We suggest that constant P(DCS) over a wider range of P2 is better described by TR's that decrease as P2 decreases, which is supported by additional data (3,5), and simulations of bubble growth from models that were not statistically optimized to data (2,8,13,14). In other words, a better calculation of decompression dose than TR will show that the same dose at two different P2's yields a lower TR at the lower P2.

We use techniques from survival analysis similar to those described by investigators in the U.S. Navy (15,18). However, we chose to integrate the hazard function from the beginning of the test at altitude to the first complaint of a symptom, without accounting for an interval of time over which the subject is defined to be free of a symptom. By definition in this application, there is no uncertainty as to when a symptom occurs since the subject is monitored in a hypobaric chamber for the duration of the test, and is instructed to report any symptom during the test.

From the Space Biomedical Research Institute, NASA/Johnson Space Center/SD5, Houston, TX (J. Conkin, M.R. Powell, P.P. Foster, J.M. Waligora); and KRUG Life Sciences, Houston, TX (K.V. Kumar).

This manuscript was received for review in April 1995. It was revised in April and May 1995, and accepted for publication in May 1995.

Address request reprints through: Space Biomedical Research Institute, NASA/Johnson Space Center/SD5, Houston, TX 77058.

We define a hazard function in terms of four variables: $P1N_2$, P2, the presence or absence of exercise at P2, and time at P2; and use the notation: h(t; z) = f(time, P2, $P1N_2$, exercise) to denote the hazard function for a decompression dose model, where (t; z) represents various combinations of the four variables and any constants. The hazard function describes the instantaneous failure rate, or the probability of failure in a small interval of time given that an individual has survived to the beginning of the interval (10).

Our approach uses an a priori definition of h(t; z) based on empirical observations of failure times and symptom intensity. In general, the onset of a symptom is not instantaneous, and the risk of having a symptom increases with time. However, it is unlikely that a person will develop a symptom if he survives past some critical time, since breathing 100% oxygen (O_2) will ultimately reduce the N_2 pressure in the tissues. Also, some people with Type I (pain only) symptoms report that the intensity of pain reaches a peak, then subsides, and in some cases is completely gone before the end of a test. Given a simple mechanical view of DCS, it is easy to envision the change in volume or deformation pressure of a gas phase in a tissue through time as the cause of the temporal onset of symptoms, intensity of symptoms, and resolution of symptoms as the person continues to denitrogenate after the decompression. In hypobaric decompressions, the instantaneous risk of DCS may increase with time, but only to a certain point in time. The observed pattern of failure time and intensity of symptoms leads us to speculate that the incidence of DCS from hypobaric decompressions might be well-described with a hazard function that rises to a peak and then decreases with time.

METHOD

The probabilistic approach to DCS modeling requires four items: a) data that consist of a dichotomous response variable and one or more explanatory variables; b) a probability function (i.e., Hill, logistic, or hazard function (6,11,18), which structures the model so that the outcome is a probability between zero and one); c) a model that calculates dose; and d) a parameter estimation routine on a computer that uses maximum likelihood. The survival analysis approach combines both probability and dose models into a single function, the survival function, without using additional parameters just for the probability transform. The aims are to: a) estimate unknown parameters in a family of models that maximize the agreement between the observed DCS incidence obtained from hypobaric chamber tests and the predicted DCS incidence from the models; and b) assess the goodness of fit of the one probability model that best fits the data.

Data and Isoprobability Isopleths

The data for this analysis are taken from 66 recent NASA and USAF research tests from about 1975 to 1990, and are available through the Hypobaric Decompression Sickness Databank (HDSD) (5). The chamber tests are not all the same in that denitrogenation periods varied, some tests used a staged decompression as part of the denitrogenation process, the breathing gas after the final decompression was not always 100% O_2, and the type

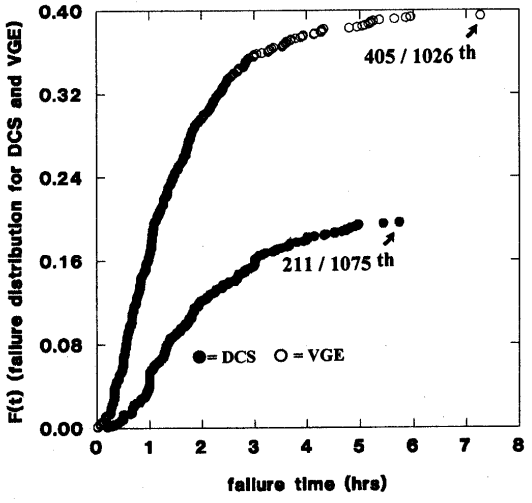

Fig. 1. The DCS and VGE failure distributions for data used in this analysis. Notice that each curve is "S" shaped, which helps to define an appropriate hazard function.

and intensity of exercise between some tests were different. In all cases, the calculation of cumulative risk began on reaching the final test altitude, and accounting for the change in tissue N_2 pressure during the final altitude exposure is not part of this modeling approach.

Of the 1075 total exposures, 863 involved repetitive, moderate exercise at P2 that is characterized predominately as upper body exercise (544 exposures). The average TR ($P1N_2$/P2) was 1.62 with a range from 0.94 to 3.46, an average P2 of 5.8 psia, and an average time at P2 of 4.75 h. There were 211 cases of DCS in 1075 exposures (20%) and 405 cases of detectable venous gas emboli (VGE) in 1026 exposures (39%), measured with a Doppler bubble detector at the precordial position. The average failure time for VGE detection was 1.5 h, and 2.0 h for volunteering DCS symptoms. Data about hypobaric decompressions in females are available in the HDSD, but were excluded from this analysis to eliminate gender as a possible source of variability in the DCS outcome.

Fig. 1 shows the failure distribution, F(t), in 211 males with DCS and 405 males with VGE. The failure distribution is the cumulative distribution of failure time divided by the total number of records in the tests (15). The failure distribution for DCS and VGE is the result of 66 unique tests done under various experimental conditions. Even though the time at altitude was as long as 13 h in one test, the last report of DCS symptoms occurred at about 6 h, and about 7 h for VGE detection. Notice the "S" shaped curves of the DCS and VGE failure distributions, which give an important clue that the mathematical form of the hazard function should provide a single maximum.

Fig. 2 is used to help describe an isoprobability isopleth. Given y = f(x), and all combinations of "x" and "y" provide the same P(DCS), then the function would define an isoprobability isopleth. The figure shows a vertical and horizontal array of 66 circles on a P2 vs. $P1N_2$ plot. The area of a circle represents the incidence of any

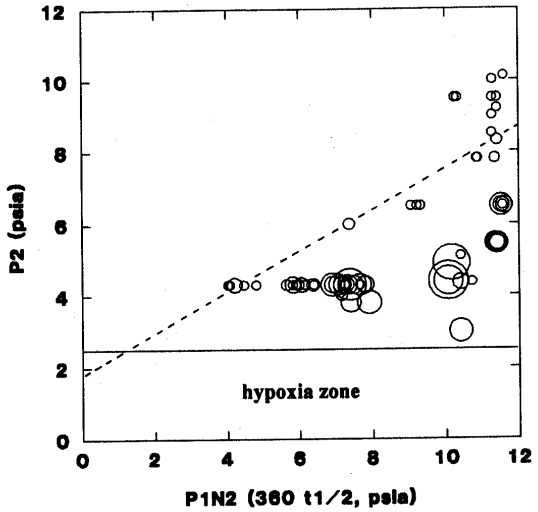

Fig. 2. The dashed line is a qualitative estimate of the zero isoprobability isopleth for data on a P2 vs. $P1N_2$ plot used in this analysis. The area of a circle is proportional to the incidence of DCS in a group. Notice that the origin (intercept) for the isopleth is on the positive P2 axis, or on the negative $P1N_2$ axis.

DCS symptom, except paresthesia, in a group of men during their stay at P2. The largest circle is 78% incidence and the smallest is a 0% incidence. Consider the vertical array of circles located between about 10.0 and 11.6 psia on the $P1N_2$-axis. Each circle represents a result from an ascent to P2 without the benefit of significant denitrogenation. Notice the area of the circles generally increase as P2 decreases at a constant $P1N_2$. Consider also the horizontal array of circles at about 4.3 psia on the P2-axis. Each of these circles represent a result from a group that ascended to about 4.3 psia, but experienced substantial denitrogenation in most cases. Notice the area of the circles also increases as $P1N_2$ increases with P2 constant at about 4.3 psia.

The dashed line on Fig. 2, the zero isoprobability isopleth, includes the approximate point in both the horizontal and vertical array of circles where the incidence of DCS just starts to increase and extrapolates to a positive P2 or negative $P1N_2$ intercept. Both horizontal and vertical arrays of data are needed to provide the minimum of 2 points required to construct the zero isoprobability line. One goal is to estimate the isoprobability isopleths for these data using an expression for decompression dose that accounts for $P1N_2$, P2, exercise, and time at P2; all structured into a probability model. Decompression dose appears as one unique slope, with all other slopes sharing a common intercept on a P2 vs. $P1N_2$ plot. Therefore, the model for dose should contain an intercept term that is estimated along with other parameters in the model. The intercept might be in one of the four quadrants, or at the origin of a P2 vs. $P1N_2$ plot, depending on the data. Finally, the horizontal solid line defines the beginning of the hypoxia zone, a region below about 2.5 psia (41,500 ft) where hypoxia is present even when 100% oxygen is delivered under positive pressure breathing. Few tests were done below 2.5 psia.

The final model received an external validation in order to assess how well the model predicts what is observed in a second, independent set of data that are substantially different from the data set used to fit the model. Data for the external validation come from 52 groups of men in the USAF who were tested from 1940 to about 1975. Of the 1009 total exposures, 575 involved repetitive exercise at P2 that is characterized predominately as lower body exercise (457 exposures). The average TR was 1.92 with a range from 0.90 to 2.98, an average P2 of 5.8 psia, and an average time at P2 of 4.66 h. There were 326 cases of DCS in 1009 exposures (32%). The average failure time was 1 h for volunteering DCS symptoms, but there were no VGE data since the instrument to detect moving gas bubbles in the blood had not yet been invented.

Denitrogenation and the 360 Min Half-Time Compartment

Prebreathing 100% O_2 or O_2-enriched mixtures prior to a hypobaric decompression is an effective and often used technique to prevent DCS (17). Therefore, it is necessary to account for the use of O_2-enriched mixtures prior to decompression in order to use the majority of information in the HDSD. The N_2 partial pressure in a tissue is an important variable in any mechanistic model about DCS. Eq. 1 defines how $P1N_2$ is calculated; it approximates a more complex process of dissolved N_2 kinetics in living tissue. Following a step-change in N_2 partial pressure in the breathing medium, such as during a switch from ambient air to a mask connected to 100% O_2, the N_2 partial pressure that is reached in a designated tissue compartment after a specific time is:

$$P1N_2 = P_0 + (P_a - P_0) * (1 - \exp^{-k*t}), \qquad \text{Eq. 1}$$

where $P1N_2$ = the N_2 partial pressure in the tissue after "t" minutes, P_0 = initial N_2 partial pressure in the compartment, P_a = ambient N_2 partial pressure in breathing medium, exp = base of natural logarithm, and t = time at the new P_a in minutes. The tissue rate constant "k" is related to the tissue N_2 half-time ($t_{1/2}$) for N_2 pressure in a compartment, and is equal to $0.693/t_{1/2}$, where $t_{1/2}$ is the 360 min tissue N_2 partial pressure half-time, and 0.693 is the natural log of two. The initial, equilibrium N_2 pressure (P_0) in the tissue at sea level is taken as 11.6 psia instead of an average alveolar N_2 pressure of 11.0 psia. The use of dry-gas, ambient N_2 pressure as equilibrium tissue N_2 pressure (P_0), and as the N_2 pressure in the breathing mixture (P_a) makes the application of Eq. 1 simple.

We use an iterative approach to select an acceptable half-time compartment. A spectrum of half-times from 300–540 min are evaluated at about 10-min intervals once a promising probability model is developed. The log likelihood (LL) for the best model in this report only improved by 0.23 units on going from a 360- to a 400-min compartment with the five parameters allowed to vary, and was much worse with faster or slower compartments. The operational relevance of the 360-min compartment is established at the Johnson Space Center, so we decided to use this compartment since there is minimal effect on the final model.

Probability Function: The Log Logistic Survival Model

A bell shape for h(t) is suspected based on the "S" shape of the DCS or VGE failure distributions in Fig. 1 because of the mathematical relationships between h(t), f(t), F(t), and S(t) (7,10). The survival function is defined as: $S(t) = 1 - F(t)$, and since the probability density function, $f(t) = dF(t)/dt$, is related to the hazard function, $h(t) = f(t)/S(t)$, the functional form of h(t) is expected to have a single maximum given F(t) from the plots of data in Fig. 1. The log logistic survival model has a h(t) with a maximum (7), and serves as the basis to subsequently define h(t; z). The Appendix contains a development of the log logistic survival model, and an example where the functional form of h(t) is retained but expanded to include a combination of variables that influence the outcome of a decompression.

Parameter Estimation by Maximum Likelihood

Maximum likelihood is the preferred method to optimize unknown parameters in a probability model where the response variable is dichotomous and the predicted value is a probability. The maximum likelihood method provides the probability that y = 1 given a value for "x", and has been clearly explained by others (11,15,18,19). The likelihood function (L) for a set of data (d + n) with some right censored times has two components, one for the failure times (set d) and the other for the censored times (set n). Denoting the failure times by t_i, i = 1, 2, . . . , d, and the censored times by t_i, i = d + 1, d + 2, . . . , n, the likelihood function is (1):

$$L = \prod_{i=1}^{d} f(t_i) * \prod_{i=d+1}^{n} S(t_i) \qquad \text{Eq. 2}$$

A person with DCS contributes a term $f(t_i)$ to the likelihood, the density of failure at t_i. The contribution from a person whose survival time is censored at t_i is $S(t_i)$, the probability of survival beyond t_i.

The log likelihood is:

$$LL = \sum_{i=1}^{d} \ln f(t_i) + \sum_{i=d+1}^{n} \ln S(t_i), \qquad \text{Eq. 3}$$

where ln is natural logarithm. Given the functional form of h(t; z), both f(t; z) and S(t; z) are derived (1,7,10) and used to define the LL function (see Appendix). The SYSTAT (ver. 5.03) Nonlin module was used to estimate unknown parameters in the models, with the summed LL minimized using the Quasi-Newton algorithm (20).

RESULTS

Table I lists the family of hazard models tested, the LL number for each, and number of fitted parameters in each model. The two parameter log logistic survival model with only failure and censored times returned a LL of −846. The ability to describe the response variable improved when h(t) was modified to h(t; z) by including 1/P2 as evident by the magnitude of the decrease in the absolute value of the LL number for the first h(t; z) model compared to the log logistic model. By accounting for denitrogenation procedures in the $P1N_2$ variable, the LL number improved, and each subsequent h(t; z) model; combinations of $P1N_2$, P2, exercise, and constants, improved the LL number.

TABLE I. LOG LIKELIHOOD OF SEVERAL MODELS

Model	LL Parameters
log logistic survival model:	
$h(t) = \lambda * (t^{\lambda-1}) * \rho^{\lambda}/[1 + (t * \rho)^{\lambda}]$	−846 2 (λ, ρ)
log logistic survival model with additional variables and constants:	
$h(t; z) = \lambda * (\text{equation}) * (t^{\lambda-1}) * \rho^{\lambda}/[1 + (\text{equation}) * (t * \rho)^{\lambda}]$	
(equation)	
1/P2	−814 2
$P1N_2/P2$	−801 2
$(P1N_2/P2) - c$	−746 3 (c = 0.97)
$[P1N_2/(P2 + c1)] - 1.0$	−742 3
$[(P1N_2 + c1)/P2] - 1.0$	−743 3
$\{[(P1N_2 + c1)/P2] - 1.0\} * [1 + (c3 * \text{exercise})]$	−738 4
$\{[P1N_2/(P2 + c1)] - 1.0\}^{c2} * [1 + (c3 * \text{exercise})]$	−667 5
$\{[(P1N_2 + c1)/P2] - 1.0\}^{c2} * [1 + (c3 * \text{exercise})]$	−663 5 Eq. 4

LL = log likelihood number.
λ, ρ, c, c1, c2, and c3 are fitted constants.

Parameter c1, the intercept point for all isoprobability isopleths on a P2 vs. $P1N_2$ plot, improved the model equally whether it was in the numerator or denominator of the modified TR expression. However, raising the modified TR term to a power (c2) and including the influence of exercise (c3) returned the lowest absolute value for the LL number when the intercept term was in the numerator. A positive value for c1 in the numerator results in an intercept on the negative $P1N_2$-axis of a P2 vs. $P1N_2$ plot. The change in LL from −738 to −663, an improvement of 75 LL units, from the addition of a power term to the modified TR with exercise was impressive, and warrants a brief comment. The link between the expansion of a gas volume in an elastic tissue and the report of a pain sensation may not be direct, or simple, and the addition of the power term provided a degree of freedom to explore this notion. However, it is also likely that the improvement in LL was due to a fortunate empirical adjustment in the hazard function and not related to our notion about gas expansion in elastic tissue.

Table II A and B lists information about the five parameters in the last h(t; z) model in Table I (Eq. 4); the model with the best fit to the data. The unitless index parameter (λ) has a value greater than 1.0, which means a plot of h(t; z) vs. time will always show a maximum, regardless of the values for $P1N_2$, P2, exercise, or time at P2. The asymptotic standard error for "λ" was small relative to the parameter estimate, therefore the ratio of the parameter estimate to the standard error was high at 17.2. The asymptotic correlation matrix (Table IIB) shows that "λ" was not highly correlated, either positively or negatively, with the other four parameters; therefore, keeping "λ" in the model was justified (20).

Fig. 3 shows various plots from Eq. 5 where "Dose"

TABLE IIA. PARAMETER ESTIMATES FOR EQUATION 4.

Parameter	Estimate	Asymptotic SE	Units	Estimate/SE
λ (index)	1.521	0.0884	dimensionless	17.20
ρ (scale)	0.063	0.0212	reciprocal of time (h^{-1})	2.95
c1 (threshold)	1.563	0.4335	pressure (psia)	3.60
c2 (power)	4.366	0.4068	dimensionless	10.73
c3 (weight factor)	1.578	0.7079	dimensionless	2.23

SE = standard error: for maximum likelihood estimation the mean square error is rescaled to one at the end of the iterations to get the correct standard errors of the parameters.

TABLE IIB. ASYMPTOTIC CORRELATION MATRIX.

	λ	ρ	c1	c2	c3
λ	1.000				
ρ	0.276	1.000			
c1	−0.070	−0.833	1.000		
c2	0.222	−0.554	0.621	1.000	
c3	0.092	−0.556	0.133	0.187	1.000

is from Eq. 6, the cumulative hazard [H(t; z)] form of Eq. 4 (see Appendix). The P(DCS) at time "t" becomes:

$$P(DCS_t) = 1 - \exp^{-Dose}, \quad \text{Eq. 5}$$

where "Dose" is:

$$H(t; z) = Dose = \ln\{1 + [((P1N_2 + c1)/P2) - 1]^{c2} \times [1 + (c3 * exercise)] * (t * \rho)^{\lambda}\} \quad \text{Eq. 6}$$

Fig. 3 shows the increase in P(DCS) with an increase in time at 3.5, 4.3, and 6.0 psia with TR = 1.65 in all cases, when exercise is (solid curves) or is not part of the test (dashed curves). The curves are examples where given the same TR, the P(DCS) at any time is always greater at a lower P2, regardless of the exercise at P2. The 95% confidence interval for one probability curve is included, and was calculated based on a propagation of errors formula (6,11). The interval provides a defined range for the estimate, but does not establish the accuracy of the estimate. In other words, it would be wrong to conclude that Eq. 6 has a superior goodness of fit based exclusively on a narrow confidence interval, since a model with a poor goodness of fit can have a narrow confidence interval if the sample size was very large (6). In this extreme case, one is very confident in the estimate of P(DCS), but the estimate is poor.

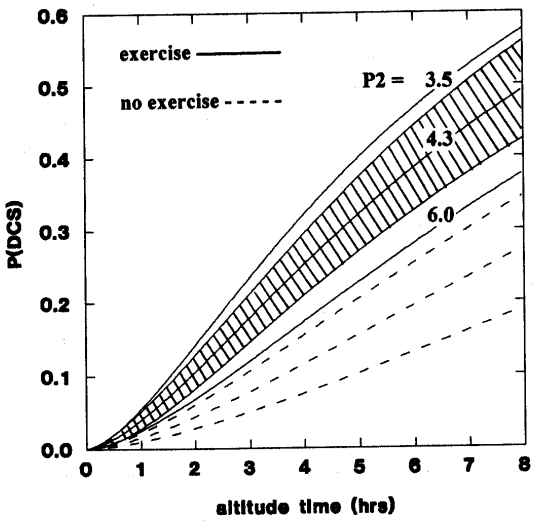

Fig. 3. The P(DCS) at either 3.5, 4.3, or 6.0 psia with (solid line) or without (dashed line) exercise at a particular time after decompression. The ratio of $P1N_2$ to P2 (TR) in Eq. 5 was 1.65 for each curve, but notice the P(DCS) increases as P2 decreases at any particular time after decompression. The 95% confidence interval is provided for the curve specific to the 4.3 psia exposure that included exercise.

A consequence of isoprobability isopleths that intercept on the negative $P1N_2$-axis of a P2 vs. $P1N_2$ plot is that constant P(DCS) is described by TR's that decrease as P2 decreases. **Fig. 4** shows 3 such isoprobability isopleths (5%, 10%, and 20%) on a TR vs. P2 plot specific to a 6-h test that included modest physical activity at P2. Notice that as P2 decreases the TR decreases to maintain the same calculated probability of DCS along a curve. For example, a 5% probability of DCS is estimated with a TR of 1.313 at a P2 pressure of 6.0 psia, and a TR of 1.210 at a P2 pressure of 4.3 psia. The calculated dose at each point along the 5% isopleth is 0.051 using Eq. 6 plus the conditions of this example.

The dark circle on Fig. 4 is the approximate location of two tests done at the Johnson Space Center (4). The observed incidence of DCS was 21% (n = 28), and 23% (n = 35) in these tests. The circle is on the 38% isopleth, and the difference between the observed DCS and the predicted DCS based on Eq. 6 is covered next. Eq. 6 is the decompression dose expression and was the best fit of the models in Table I regardless of the strength of the relationship between the dependent and independent variables. Goodness of fit, after obtaining the model with the best fit, is a measure or impression of agreement between the predicted outcome and the observed outcome. Without an assessment of goodness of fit it is possible to be unjustifiably confident in a calculation of P(DCS).

DISCUSSION

Goodness of Fit

Statistical confidence in an estimate of P(DCS) is based on the goodness of fit, and **Fig. 5** graphically shows the

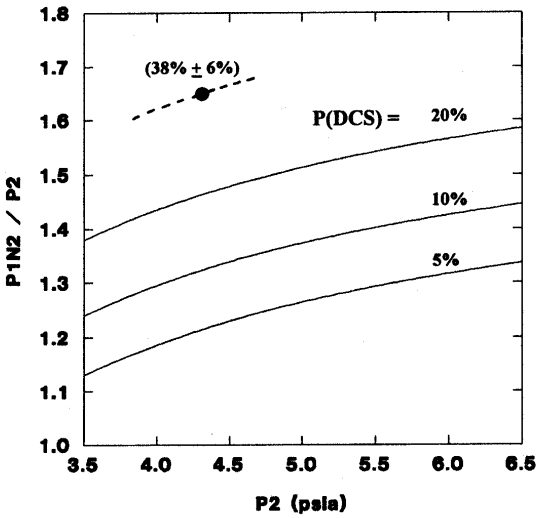

Fig. 4. Three isoprobability isopleths on a TR vs. P2 plot that are specific to a 6-h test that included exercise. Notice that as P2 decreases, TR decreases to maintain a constant P(DCS) on each curve. The dark circle on the 38% isopleth is the location of specific NASA testing that resulted in about a 22% incidence of decompression sickness.

goodness of fit of Eq. 5. The observed DCS incidence in 66 groups is compared to the predicted DCS incidence from Eq. 5, which was based on the 1075 exposures in the 66 tests. The area of a circle is proportional to the number of people in a test. The smallest area indicates one person in a test, and the largest area indicates 82 people in a test. Data from tests with large number of people contribute more to the model, so larger circles are located nearer to the identity line in Fig. 5.

The position of all the circles on Fig. 5 gives an impression of a reasonable fit of Eq. 5, given the simple formulation of the model, the realization that random variability in the outcome will never be completely managed, and the limitation of Fig. 5 to provide an assessment of goodness of fit. Goodness of fit based on group incidence is limited because the precision of group incidence is greatly influenced by the number of people in a group. The predicted incidence of DCS in 36 of the 66 groups (55%) was within 0.05 above or below the observed incidence, while 47 groups (71%) had a predicted incidence within 0.10 above or below the observed incidence. Three NASA tests, seen as dark circles on Fig. 5, are included in the 19 groups (29%) that had a predicted incidence greater than 0.10 above or below the observed incidence. Two of these tests are discussed to show how conflicting data or an incomplete model can decrease the goodness of fit of the model to the data. Both tests included a 30-min decompression to 4.3 psia for 6 h with a TR of 1.60. The first, the smaller of the two dark circles above the identity line on Fig. 5, included exercise after the decompression and had a 21% incidence of DCS (6 cases in 28 exposures). The second, the dark circle below the identity line, did not include exercise after the decompression and had a 41% incidence of DCS (7 cases in 17 exposures). These results conflict, since a greater incidence of DCS under sedentary conditions in otherwise similar tests is not the observed trend in the entire data set. Eq. 5 calculates a P(DCS) for the group with exercise as 0.33 and as 0.16 for the group without exercise, and even though the trend in the entire data set is reflected in the P(DCS) calculations, the two probabilities are different by more than 0.10 of the observed incidence, thus reducing the goodness of fit.

Another approach to assess goodness of fit is to compare the LL numbers for 3 models: the 1 variable-2 parameter log logistic model (LL = −846), the 4 variable-5 parameter continuous model (Eq. 5 with a LL = −663), and the 66 parameter discontinuous model (LL = −342). The log logistic model with just time as a variable has a poor LL, and the discontinuous model has the best LL based on the definition that the observed P(DCS) for the 66 tests is the true P(DCS) (19). The continuous model would not necessarily predict in all cases the observed P(DCS) in the 66 tests, so the LL for the continuous model would always exceed that of the discontinuous model. There was a 36% improvement [100 * (846 − 663)/(846 − 342)] in Eq. 5 over the log logistic model using this approach; a substantial improvement but a better model might be developed.

To improve the goodness of fit, the data might be further screened to control for additional experimental variables, such as time of ascent, which is about 10 min for the entire data set but about 30 min for the three tests seen as dark circles on Fig. 5. The slow rate of ascent in the two tests seen as dark circles above the identity line could have contributed to fewer cases of DCS than predicted by Eq. 5, and Eq. 5 would be more complete by

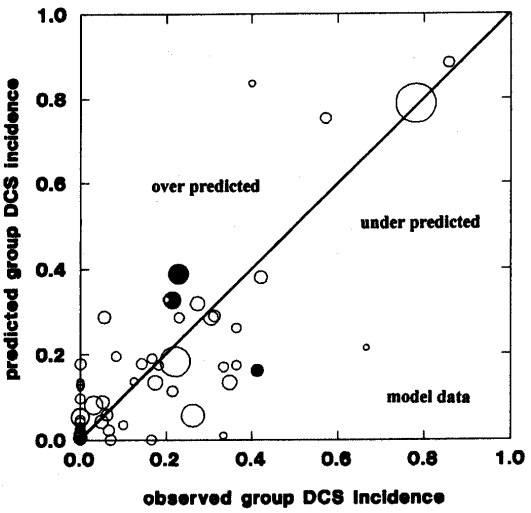

Fig. 5. Predicted vs. observed DCS incidence in 66 groups used to fit Eq. 5. The area of a circle is proportional to the number of people in a group. The three dark circles are results from NASA tests at 4.3 psia with TRs between 1.60 and 1.65 where exercise is (2 circles above identity line) and is not (circle below identity line) part of the test (4). The model neither over or under estimates the entire data set, but did over estimate the incidence of DCS in several small groups that reported no symptoms.

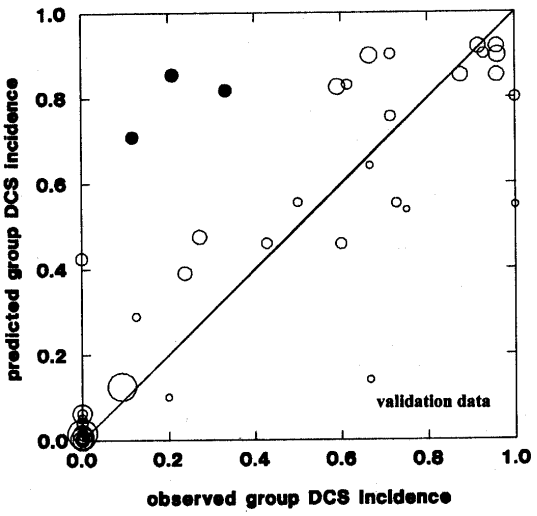

Fig. 6. Validation of Eq. 5 by using it to predict the DCS incidence in 52 groups not used to fit Eq. 5. The plot shows a comparison of the predicted to the observed DCS incidence in the groups. The three dark circles are tests where the predicted incidence is much more than the observed incidence, and are used to discuss bias in reporting DCS symptoms (see Discussion).

including time or rate of ascent. Finally, tests might be eliminated where bias in over- or under-reporting mild symptoms is suspected, which is always a concern.

External Validation

External validation of the model was done by comparing the predictions of Eq. 5 to the observed outcomes in a second, independent set of data (see Methods). **Fig. 6** shows how well the model predicted the observed DCS from a second data set. Except for three cases identified as dark circles on Fig. 6, the predictions from the model generally agree with the observations in the validation data set, or at least as well as in the model data set. There are two notable differences between the two data sets that could reduce the goodness of fit of the model to the validation data set: a) lower body exercise was the dominant type of activity in the validation data set while upper body exercise was the dominant activity in the model data set; and b) the validation data set included results collected prior to and during World War II, while the model data set is more contemporary. The "historical" validation data might be biased in that mild symptoms of DCS may not have been volunteered in all cases. For example, the three dark circles in Fig. 6 are tests where the observed incidence of DCS is substantially less than the predicted incidence from the model. These were tests to about 3.0 psia for 2–4 h. There were 54 total exposures, and 12 cases of DCS of which 11 cases were severe enough to cause the test to be stopped before the scheduled end of the test. The three chamber tests are described in reports from 1942–45 where O_2 prebreathing procedures were being evaluated as to their effectiveness in preventing DCS during high-altitude bombing missions. These tests had a very high abort rate (11/12, 92%), and it is likely that the incidence of less severe symptoms in the remaining subjects would be higher. A bias in not reporting mild symptoms seems evident in these tests, and is understandable since the requirement was to develop an operational high-altitude bombing program.

Metabolic Gases and Hypobaric Decompression Sickness

The best fit to the data was with an intercept for all isoprobability isopleths on the negative $P1N_2$-axis of a P2 vs. $P1N_2$ plot. The intercept has no particular physiological or mechanistic meaning; it is just the origin of the extrapolated isopleths. However, it could be a consequence of the combined contributions of: a) the limiting boundaries of the decompression test envelope (i.e., the hypoxia zone); b) an artifact established by the $P1N_2$ calculation since the horizontal position on Fig. 2 of a group test after O_2 prebreathing is determined by the half-time compartment; c) the influence of exercise in the genesis and growth of bubbles; and d) the contribution of metabolic gases to hypobaric DCS (13,14), which can only be inferred from a P2 vs. $P1N_2$ plot. Isopleths that have a negative $P1N_2$ intercept all cross at unique positive P2 values on the P2 axis when $P1N_2$ is zero, indicating that there is risk of DCS even though N_2 is not available in the 360-min compartment. The positive P2 intercepts for the isopleths may be an indication that metabolic gases have a significant role in hypobaric DCS. Even in a tissue devoid of all dissolved N_2, the dissolved metabolic gases and water in the tissue would come out of solution (ebullism) as ambient pressure approaches a vacuum.

In conclusion, Eq. 5 serves as a guide to quantify how manipulation of four variables before and after the decompression can change the P(DCS) so that an acceptable level of risk is achieved. The acceptable level of risk is debatable; it depends on many factors such as the importance of success for a particular mission, or the availability of DCS treatment. A model based only on four variables and fitted to a limited amount of similar research data will not adequately predict the risk of DCS for all possibilities of hypobaric decompressions. For example, this model would not be useful with very slow or rapid ascents, or if the partial pressure of N_2 in the breathing mixture was changing slowly in time. However, combining a few important variables into an abstraction of the true decompression dose that is then statistically optimized to a DCS response is a practical means to model hypobaric DCS. As more and better-described data become available, this approach will continue to provide a powerful tool to assess the risk of hypobaric DCS.

APPENDIX: MODIFIED LOG LOGISTIC SURVIVAL MODEL

The hazard function [h(t)] for the log logistic survival model is:

$$h(t) = \lambda * (t^{\lambda-1}) * \rho^{\lambda}/[1 + (t * \rho)^{\lambda}] \qquad \text{Eq. 1A}$$

where λ and ρ are index (unitless) and scale (hr^{-1}) parameters to be estimated, respectively, and "t" is time in hours in this application. When $\lambda > 1.0$, the h(t) has a maximum, and resembles a bell shape (7).

The cumulative hazard function, [H(t)], follows from the integration of h(x) over a specific time "t", the time at P2 in this application:

$$H(t) = \int_0^t h(x)\,dx \qquad \text{Eq. 2A}$$

where "x" can be time. Note that h(t) may not vary with time, as with the exponential model (7), but the integral of h(t) will give H(t) in terms of the starting and ending time at P2. A combination of Eq. 1A and Eq. 2A yields:

$$H(t) = \ln [1 + (t * \rho)^{\lambda}] \qquad \text{Eq. 3A}$$

where ln is natural logarithm, and since the survival function [S(t)] is also defined as:

$$S(t) = \exp^{-H(t)} \qquad \text{Eq. 4A}$$

the S(t) from Eq. 3A and Eq. 4A for the log logistic model becomes:

$$S(t) = 1/[1 + (t * \rho)^{\lambda}] \qquad \text{Eq. 5A}$$

and since the probability density function [f(t)] is:

$$f(t) = h(t) \exp^{-H(t)} \qquad \text{Eq. 6A}$$

the f(t) from Eq. 1A and Eq. 3A for the log logistic model is:

$$f(t) = \lambda * (t^{\lambda-1}) * \rho^{\lambda}/[1 + (t * \rho)^{\lambda}]^2 \qquad \text{Eq. 7A}$$

The P(DCS) at time "t" based only on failure and censored times becomes:

$$P(DCS_t) = 1 - \exp^{-H(t)} \qquad \text{Eq. 8A}$$

The functional form of h(t) is retained but is expanded to include combinations of three variables besides time that influence the outcome of the decompression: $P1_{N_2}$, P2, and exercise. The gas phase contribution to h(t) could be as simple as 1/P2, or as complex as $[((P1_{N_2} + c1)/P2) - 1]^{c2}$, but the exercise contribution is always in the form [1 + (c3 * exercise)], where exercise at P2 is one or zero, and c1, c2, and c3 are estimated parameters.

The h(t; z) for a simple modification of the log logistic model that includes P2 and exercise becomes:

$$h(t; z) = \lambda * (1/P2)^{c2} * [1 + (c3 * \text{exercise})] * (t^{\lambda-1}) * \rho^{\lambda}/$$
$$\{1 + (1/P2)^{c2} * [1 + (c3 * \text{exercise})] * (t * \rho)^{\lambda}\} \qquad \text{Eq. 9A}$$

The H(t; z) from Eq. 2A and Eq. 9A becomes an expression of decompression dose as a function of 3 variables associated with DCS plus the fitted parameters that maximize the agreement between dose and response:

$$H(t; z) = \text{Dose}$$
$$= \ln \{1 + (1/P2)^{c2} * [1 + (c3 * \text{exercise})] * (t * \rho)^{\lambda}\}, \qquad \text{Eq. 10A}$$

and the P(DCS) at time "t" based on P2, exercise, and time at P2; both failure and censored times, becomes:

$$P(DCS_t) = 1 - \exp^{-\text{Dose}}. \qquad \text{Eq. 11A}$$

ACKNOWLEDGMENTS

We thank Hugh D. Van Liew from the Department of Physiology, SUNY at Buffalo, and Mark E. Burkard from the University of Rochester School of Medicine for their consultations, which established the foundation of this report.

REFERENCES

1. Brown Jr. BW. Estimation in survival analysis: parametric models, product-limit and life-table methods. In: Mike V, Stanley KE, eds. Statistics in medical research. New York: John Wiley and Sons, 1982: 317–39.
2. Burkard ME, Van Liew HD. Simulation of exchanges of multiple gases in bubbles in the body. Respir Physiol 1994; 95:131–45.
3. Chadov VI, Iseyev LR. Variations in the maximal allowable supersaturation coefficient during altitude decompression. Kosm Biol Aviak Med 1989; 23:58–62. [English Abstract In: Hooke LR, Teeter R, Donaldson PL, ed. USSR space life sciences digest. NASA CR-3922(28), Issue 24, Springfield, VA: National Technical Information Service, 1989: 94–5.]
4. Conkin J, Edwards BF, Waligora JM, Stanford Jr. J, Gilbert III JH, Horrigan Jr. DJ. Updating empirical models that predict the incidence of aviator decompression sickness and venous gas emboli for Shuttle and Space Station extravehicular operations. Houston: Johnson Space Center, 1990; NASA Technical Memorandum 100456 Update.
5. Conkin J, Bedahl SR, Van Liew HD. A computerized databank of decompression sickness incidence in altitude chambers. Aviat Space Environ Med 1992; 63:819–24.
6. Conkin J. Probabilistic modeling of hypobaric decompression sickness [Dissertation]. Buffalo, NY: State University of New York at Buffalo, 1994.
7. Cox DR, Oakes D. Analysis of survival data. New York: Chapman and Hall, 1984: 13–21.
8. Gernhardt ML. Development and evaluation of a decompression stress index based on tissue bubble dynamics [Dissertation]. Philadelphia, PA: University of Pennsylvania, 1991.
9. Kumar KV, Powell MR. Survivorship models for estimating the risk of decompression sickness. Aviat Space Environ Med 1994; 65:661–5.
10. Lee ET. Statistical methods for survival data analysis, 2nd ed. New York: John Wiley and Sons, 1992: 8–18.
11. Van Liew HD, Conkin J, Burkard ME. Probabilistic model of altitude decompression sickness based on mechanistic premises. J Appl Physiol 1994; 76:2726–34.
12. Van Liew HD, Burkard ME. Density of decompression bubbles and competition for gas among bubbles, tissue and blood. J Appl Physiol 1993; 75:2293–301.
13. Van Liew HD, Burkard ME. Simulation of gas bubbles in hypobaric decompressions: roles of O_2, CO_2, and H_2O. Aviat Space Environ Med 1995; 66:50–5.
14. Van Liew HD, Burkard ME. Simulation of gas bubbles and the role of O_2, CO_2, and H_2O. Undersea and Hyperbaric Med 1994; 21(15, Suppl.):20.
15. Vann RD, Thalmann ED. Decompression physiology and practices. In: Bennett PB, Elliott DH, eds. The physiology and medicine of diving, 4th ed. Philadelphia, PA: W.B. Saunders, Ltd., 1993: 397–406.
16. Vann RD. A likelihood analysis of decompression data using Haldane and bubble growth models. In: Bove AA, Bachrach AJ, Greenbaum Jr. LJ, eds. Proceedings of 9th International Symposium of Underwater and Hyperbaric Physiology. Bethesda, MD: Undersea and Hyperbaric Medical Society, 1987: 165–81.
17. Waligora JM, Horrigan Jr. DJ, Conkin J. The effect of extended O_2 prebreathing on altitude decompression sickness and venous gas bubbles. Aviat Space Environ Med 1987; 58(9, Suppl.):A110–2.
18. Weathersby PK, Survanshi SS, Homer LD, Parker E, Thalmann ED. Predicting the time of occurrence of decompression sickness. J Appl Physiol 1992; 72:1541–8.
19. Weathersby PK, Homer LD, Flynn ET. On the likelihood of decompression sickness. J Appl Physiol 1984; 57:815–25.
20. Wilkinson L. SYSTAT: the system for statistics. Evanston, IL: SYSTAT Inc., 1990: 342–87.